



## Isomers and excitation modes in the gamma-soft nucleus $^{192}\text{Os}$

G.D. Dracoulis<sup>a,\*</sup>, G.J. Lane<sup>a</sup>, A.P. Byrne<sup>a</sup>, H. Watanabe<sup>a,b,1</sup>, R.O. Hughes<sup>a,2</sup>, F.G. Kondev<sup>c</sup>, M. Carpenter<sup>d</sup>, R.V.F. Janssens<sup>d</sup>, T. Lauritsen<sup>d</sup>, C.J. Lister<sup>d</sup>, D. Seweryniak<sup>d</sup>, S. Zhu<sup>d</sup>, P. Chowdhury<sup>e</sup>, Y. Shi<sup>f</sup>, F.R. Xu<sup>f</sup>

<sup>a</sup> Department of Nuclear Physics, R.S.P.E., Australian National University, Canberra, A.C.T. 0200, Australia

<sup>b</sup> RIKEN Nishina Center, 2-1 Hirosawa, Wako, Saitama 351-0198, Japan

<sup>c</sup> Nuclear Engineering Division, Argonne National Laboratory, Argonne, IL 60439, USA

<sup>d</sup> Physics Division, Argonne National Laboratory, Argonne, IL 60439, USA

<sup>e</sup> Department of Physics, University of Massachusetts Lowell, Lowell, MA 01854, USA

<sup>f</sup> School of Physics, Peking University, Beijing 100871, China

### ARTICLE INFO

#### Article history:

Received 26 December 2012

Received in revised form 12 February 2013

Accepted 13 February 2013

Available online 16 February 2013

Editor: D.F. Geesaman

### ABSTRACT

New spectroscopic results for high-spin states in  $^{192}\text{Os}$  populated in deep-inelastic reactions include the identification of a 2-ns,  $12^+$  isomeric state at 2865 keV and a 295-ns,  $20^+$  state at 4580 keV and their associated  $\Delta J = 2$  sequences. The structures are interpreted as manifestations of maximal rotation alignment within the neutron  $i_{13/2}$  and proton  $h_{11/2}$  shells at oblate deformation. Rotational band members based on the long-lived,  $K^\pi = 10^-$  isomer are also identified for the first time. Configuration-constrained, potential-energy-surface calculations predict that other prolate multi-quasiparticle high- $K$  states should exist at low energy.

© 2013 Elsevier B.V. All rights reserved.

The structure of the stable even–even isotopes of osmium,  $^{188}\text{Os}$ ,  $^{190}\text{Os}$  and  $^{192}\text{Os}$  is of considerable interest because these nuclei fall in the transitional region where static and dynamic effects due to the triaxial degree of freedom are expected to be important. Their description is challenging for theoretical models and also for experiment since signatures of triaxiality are not simple in realistic cases. The seminal Coulomb excitation studies of Wu et al. [1,2] that exploited model-independent sum rules [3], concluded that the ground-state and vibrational bands of the stable osmium nuclei have properties that fall between the predictions of  $\gamma$ -rigid or  $\gamma$ -soft models. Observables such as  $E2$  moments are reasonably well-localised, with  $^{190}\text{Os}$  and  $^{192}\text{Os}$  having average asymmetry angles close to  $20^\circ$  and  $24^\circ$  respectively [2], approaching the midpoint between prolate deformation ( $\gamma = 0^\circ$ ) and oblate deformation ( $\gamma = 60^\circ$ ). The  $N = 116$  isotope,  $^{192}\text{Os}$  also has the lowest-lying  $\gamma$ -vibrational band in the region, at 489 keV.

More recent theoretical studies include models of gamma-vibrations and static triaxiality [4–7] and extensive mean field calculations that aim to describe ground- and excited-state shape evolution [8–12] across a wide range of neutron-rich Hf, W, Os and

Pt nuclei. In a specific prediction, Walker and Xu [13] proposed that a rotation-aligned oblate structure would compete with the (largely) prolate structures in the isotones  $^{190}\text{W}$  and  $^{192}\text{Os}$  because the Fermi surface is close to the low- $\Omega$  Nilsson orbitals within the  $i_{13/2}$  neutron shell at oblate deformation (thus maximising Coriolis effects), but near the high- $\Omega$  orbitals at prolate deformation. Both situations (illustrated schematically in Ref. [14]) could result in low-lying  $12^+$  states, with the prolate case likely to be a  $K$ -isomer, as will be discussed later. The underlying issue for all these approaches is that in soft nuclei in particular, the resultant behaviour is likely to be configuration-dependent.

Experimentally, isomers can be a boon since they enable high spectroscopic sensitivity, temporal ordering of transitions within a nucleus, and in principle they provide a signature of specific deformations through the identification of characteristic orbitals near the Fermi surface [14].  $K$ -isomers occur in well-deformed nuclei when the orbitals have large angular momentum projections,  $\Omega_i$  on the nuclear symmetry axis. By combining them, low-energy states with a large total projection  $K = \sum \Omega_i$  can be formed. If the  $\gamma$ -ray multipolarity  $\lambda$  of their decay fails to meet the difference in  $K$  between the initial and final states, leading to a shortfall or “forbiddenness”  $\nu = \Delta K - \lambda$ , the transitions are expected to be profoundly hindered. Long lifetimes also occur when low energies and/or high multipolarities are involved or when the transitions are associated with extensive configuration changes (see, for example [14,15]).

The presence or absence of isomers, and whether they have short or long lifetimes, is not by itself, a sign of either the validity

\* Corresponding author.

E-mail address: [george.dracoulis@anu.edu.au](mailto:george.dracoulis@anu.edu.au) (G.D. Dracoulis).

<sup>1</sup> Present address: School of Physics and Nuclear Energy Engineering, Beihang University, Beihang 100191, China.

<sup>2</sup> Present address: Dept of Physics, University of Richmond, 28 Westhampton Way, Richmond, VA 23173, USA.

**Table 1**  
Selected isomers and hindered transitions in  $^{190}\text{Os}$  and  $^{192}\text{Os}$  including results from the present work.

$E_\gamma$ (keV)	$I_\gamma$ (rel.)	Final state	$\sigma\lambda$	$\alpha_T^a$	Strength (W.u.)	$\nu$	$f_\nu$
$^{190}\text{Os}$							
	$[E = 1705 \text{ keV}; K^\pi = 10^-; \tau = 14.0(14) \text{ m}]$						
38.9	1000(2) <sup>b</sup>	$8^+_{\text{g}}$	M2	1050	$1.39(6) \times 10^{-8}$	8	9.6
	8.8(20) <sup>b</sup>		E3	24900	$4.9(11) \times 10^{-5}$	7	4.1
$^{192}\text{Os}$							
	$[E = 2015 \text{ keV}; K^\pi = 10^-; \tau = 8.5(14) \text{ s}]$						
307.0	13.3(3)	$8^+_{\text{g}}$	M2	0.975	$4.0(7) \times 10^{-9}$	8	11.2
302.5	100(6)	$7^+_{K=2}$	E3	0.433	$2.1(4) \times 10^{-4}$	5	5.4
47.4	0.0031(6)	$7^+_{K=4}$	E3	7760	$2.8(7) \times 10^{-3}$	3	7.1
	$[E = 2865 \text{ keV}; I^\pi = 12^+; \tau = 2.0(4) \text{ ns}]$						
111.5	35(6)	$10^+_{\text{(obl.)}}$	E2	2.82	9.7(26)	0	
445.7	161(5)	$10^+_{\text{g}}$	E2	0.030	$4.4(9) \times 10^{-2}$		
849.0	26(6)	$10^+_{K=10}$	M2	0.0435	$3.0(9) \times 10^{-2}$	0	
497.8	924(11)	$11^+_{K=10}$	E1	0.0077	$8.4(17) \times 10^{-7}$	1	$1.2 \times 10^6$
114.7	35(7)	$12^-_{K=10}$	E1	0.275	$2.6(7) \times 10^{-6}$	1	$3.8 \times 10^5$
	$[E = 4580 \text{ keV}; I^\pi = 20^+; \tau = 295(10) \text{ ns}]$						
85.3	100	$20^+$	E2	8.43	0.99(4)		

<sup>a</sup> BRICC, Ref. [16].

<sup>b</sup> Component intensities deduced from the known mixing ratio.

of the  $K$ -quantum number or the dilution that might occur when the deformation becomes less well-defined. The inhibition of the transition-strength represents a more quantitative probe. This hindrance ( $F$ ) is given by the inverse of the transition-strength, or equivalently, the ratio of the partial  $\gamma$ -ray lifetime compared to the Weisskopf estimate, so that  $F = \tau_\gamma/\tau_W$ . In well-deformed nuclei, the hindrance is found to scale with the forbiddenness so that the reduced hindrance  $f_\nu = F^{1/\nu}$  is approximately a constant, of magnitude  $\sim 100$ . As a result, experimental  $f_\nu$  values of this order are taken as indicators of the “goodness” of  $K$ , although lower values of  $f_\nu$  often occur because of known rotational effects and, occasionally, through random state-mixing (see [17] for examples of both).

The expectation that isomerism will diminish as the perimeter of the well-deformed region is crossed obviously needs to be treated with caution. In  $^{190}\text{Os}$  and  $^{192}\text{Os}$ , for example, despite evidence for gamma-softness, isomers with very long lifetimes are known and attributed to the  $K^\pi = 10^- \nu 11/2^+$  [615],  $9/2^-$  [505] (prolate) configuration. The  $10^-$  state at 2015 keV in  $^{192}\text{Os}$  has a meanlife of 9 s, and its counterpart at 1705 keV in  $^{190}\text{Os}$  has a meanlife of 14 min. The equivalent  $10^-$  state in  $^{194}\text{Os}$  has not, thus far, been found, consistent with theoretical predictions that it will rise quickly with neutron number (see below). The decay strengths extracted from the known properties [18,19] are listed in Table 1, together with selected results for the isomers assigned in the present study. The long lifetimes in the  $10^-$  cases arise largely because of the high multiplicities (M2 and E3) of the associated transitions.  $K$ -hindrance is still a factor, but the reduced hindrances are all anomalously low ( $\leq 10$ ), as has been found recently in our parallel studies of the neutron-rich tungsten nuclei [20]. High multiplicities have also been implicated in the formation of long-lived (triaxial) isomers in the nearby iridium isotopes [21].

Despite continuing theoretical interest, the proximity of nuclei in this region to the stability line has meant that experimental high-spin spectroscopic information has remained limited. The isotope  $^{188}\text{Os}$ , reachable by incomplete fusion, is the heaviest for which a comprehensive level scheme has been obtained [22]. However, with the development of deep-inelastic and fragmentation reactions for spectroscopic studies, both stable and neutron-rich isotopes are becoming accessible, although the results to date have been somewhat fragmentary. In the osmium cases, the ground-state bands in  $^{188}\text{Os}$ ,  $^{190}\text{Os}$  and  $^{194}\text{Os}$  have been studied [23,24]. States in  $^{194}\text{Os}$  have also been populated indirectly through the

$\beta$ -decay of the neutron-rich isotope  $^{194}\text{Re}$  [25,26] excited in fragmentation, and fragmentation was again used to identify some yrast states in  $^{198}\text{Os}$  [27]. For  $^{192}\text{Os}$ , the most recent compilation [19] records results from Ref. [28] including evidence for an isomer and the tentative placement of high-spin transitions.

From our systematic studies of stable and neutron-rich nuclei using deep-inelastic reactions, detailed spectroscopic results have now been obtained for a range of osmium isotopes. The focus of the present report will be on  $^{192}\text{Os}$ , informed as well by new results for  $^{190}\text{Os}$  and  $^{194}\text{Os}$ . (A more comprehensive report covering this range of isotopes will be presented in due course [30].) The experimental results are complemented by multi-quasiparticle calculations that include triaxiality.

As in our earlier measurements, 6.0 MeV per nucleon  $^{136}\text{Xe}$  beams were provided by the ATLAS facility at Argonne National Laboratory. Nanosecond pulses, separated by 825 ns, were incident on two targets, an enriched metallic  $^{186}\text{W}$  foil,  $\sim 6 \text{ mg/cm}^2$  thick with a 25  $\text{mg/cm}^2$  gold foil directly behind and a pressed 44  $\text{mg/cm}^2$  enriched  $^{192}\text{Os}$  target with a 10  $\text{mg/cm}^2$  gold foil behind. Gamma rays were detected with the Gammastore array [29], with 100 detectors in operation. Triple coincidences were required and the main data analysis was carried out with  $\gamma$ - $\gamma$ - $\gamma$  cubes with various time-difference conditions, and also with time constraints relative to the pulsed beam to select different out-of-beam regimes.

A partial level scheme is given in Fig. 1. (For simplicity, the energies and intensities of transitions within the  $K^\pi = 2^+$ ,  $\gamma$ -band are not shown, and numerous other non-yrast structures that were observed are not included.) Both the  $\gamma$ -band and the  $K = 4^+$  band at 1070 keV (not in the figure) are confirmed and marginally extended. Compared to what was known previously for the ground-state band [1,19], the placement of the 791-keV  $\gamma$  ray assigned as the  $12^+ \rightarrow 10^+$  transition is confirmed, although we do not have independent information that would confirm its multipolarity. The 685-keV transition assigned in Ref. [1] as a decay from a 3104-keV state was not seen in the present study but a new 752-keV transition, of marginally higher intensity than the 791-keV  $\gamma$  ray, is placed in parallel to the 791-keV transition, from a state at 3171 keV. The fact that the 752-keV transition was not observed in the Coulomb excitation study of Ref. [1] implies that it is not of (enhanced)  $E2$  multipolarity, hence the suggested spin-11 assignment for the 3171-keV state.

The lifetime of 295(10) ns for the 4580-keV state agrees with the less precise value of the (unplaced) isomer reported earlier



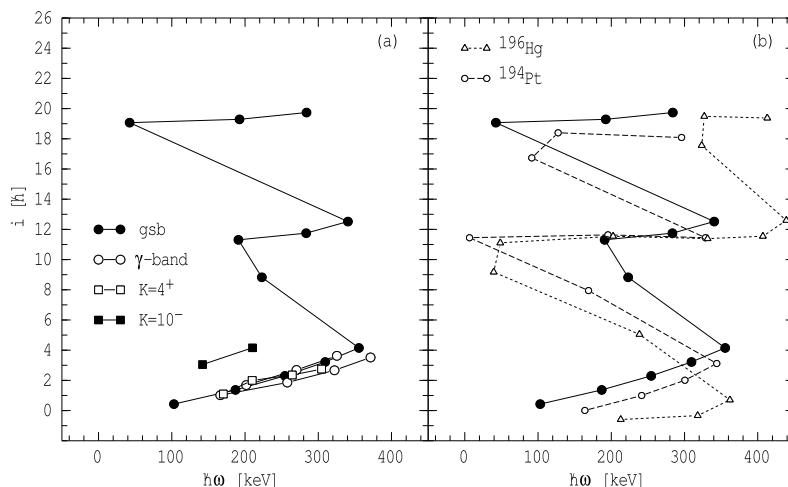


Fig. 3. (a) Net alignments for bands in  $^{192}\text{Os}$ . (b) Comparison of net alignment curves for the isotones  $^{192}\text{Os}$ ,  $^{194}\text{Pt}$  and  $^{196}\text{Hg}$ , with a common reference.

can be associated with cascades within numerous complementary partners. This includes the 668-keV line, most of whose intensity can now be attributed to known lines in  $^{130}\text{Xe}$  and  $^{132}\text{Xe}$ , although in a preliminary report [35], we placed it as a possible  $26^+ \rightarrow 24^+$  transition in  $^{192}\text{Os}$ .

There is evidently a significant difference between the probability for excitation of the complementary partners when gating on the lowest ground-state band members, compared to the situation where much higher-spin states, those above the 295-ns isomer, are selected. This can be attributed to the fact that the low-spin collective states can be populated by both inelastic scattering and multiple Coulomb excitation of the target nucleus, whereas higher spins and excitation energies require a more complex and energetic process. The spectrum in Fig. 2(d) has lines from decays in  $^{136}\text{Xe}$  (the most prominent of which, at 1313 keV, is beyond the range of the figure), but these are somewhat reduced because strong population occurs of the  $6^+$   $\mu\text{s}$  isomer in  $^{136}\text{Xe}$ , which will not be seen in prompt coincidence. In contrast, the complementary partners observed in Fig. 2(a) involve multiple neutron emissions and, therefore, much high energy input, even though significant excitation energy is required to access the high-spin states in  $^{192}\text{Os}$  itself. The deep-inelastic component of the process is apparently being selected rather than the quasi-elastic one. (See Ref. [28] for an example of these components in a comparable reaction.)

As well as the higher-lying isomer, a feature of the scheme is the 2-ns,  $12^+$  state at 2865 keV which has several decay paths, including  $E2$  transitions to two  $10^+$  states, but a dominant decay via an  $E1$  transition of 498 keV to the  $11^-$  state of the  $10^-$  band. The strengths of these branches (Table 1) will be discussed below. Important elements in the proposed spin assignments include the large total conversion coefficients deduced from intensity balances that suggest  $M1$  or  $E2$  multiplicities for the 85-keV and 112-keV transitions (as implied by the low  $\gamma$ -ray intensities in Fig. 2(b)) and in the case of the 2753-keV state, the 1044-keV branch to the  $8^+$  yrast state that would preclude an  $11^+$  alternative.

Gated angular distributions were also used to constrain spins. The angular distribution for the relatively strong 334-keV  $\gamma$  ray (Fig. 2(d)) depopulating the promptly-fed 2753-keV state has a large and positive  $A_2/A_0$  coefficient when fitted to the function  $W(\theta) = 1 + A_2/A_0 \times P_2(\cos\theta)$ , suggesting a  $J \rightarrow J$  transition, supporting the proposed  $10^+$  assignment. Most of the other transitions of interest below the 4580-keV state were found to be essentially isotropic, due presumably to relaxation, hence the tentative spins above the  $12^+$  state at 2865 keV. Note however that parallel decays such as a  $3814 \rightarrow 2865$ -keV branch were not observed,

consistent with the assumed stretched  $E2$  character for the main cascade.

The net alignments of the band structures are illustrated in Fig. 3(a). For the discussion, these have been evaluated using a reference with a lower moment-of-inertia than would be used for a prolate deformation, as is appropriate for oblate rotation. Because of this, while they are essentially the same, the low-frequency trajectories of the ground-band,  $\gamma$ -band and  $K = 4^+$  band have a small, but artificial upward slope. The  $10^-$  band shows about  $3\hbar$  more alignment, consistent with the presence of the  $11/2^+[615]$ ,  $i_{13/2}$  neutron orbital in its configuration, and there are two sharp increments in the yrast sequence, beginning near the  $12^+$  and  $20^+$  states, corresponding to alignment gains of  $\sim 12\hbar$  and  $\sim 8\hbar$  respectively. The main sequence is compared with that of the isotones  $^{194}\text{Pt}$  and  $^{196}\text{Hg}$  [32]. Most of the yrast sequence for  $^{194}\text{Pt}$  proposed by Jones et al. [31] and interpreted as being of oblate collectivity, has been confirmed in the present measurements, but some experimental modifications were necessary and are reflected in Fig. 3(b).

The comparison between these cases is suggestive: very similar alignment gains are observed within the  $\Delta J = 2$  sequences. The first is consistent with the so-called,  $AB$  alignment (see Ref. [33] for nomenclature) expected for the  $i_{13/2}$  neutron shell when the Fermi level is close to the low- $\Omega$  orbitals, as is the case for oblate deformation, and predicted for the  $^{192}\text{Os}$  case in Ref. [13]. The second gain corresponds either to alignment of the  $BC$  neutrons or possibly the  $ab$  protons, as will be discussed later. Successive  $AB$  and  $CD$  alignments is the currently accepted interpretation for  $^{196}\text{Hg}$  [32].

At the first alignment, short-lived  $12^+$  isomers resulting from low-energy  $E2$  transitions with enhanced strengths occur in both  $^{194}\text{Pt}$  and  $^{196}\text{Hg}$  [34], comparable to the isomer in  $^{192}\text{Os}$ . As listed in Table 1, the 111.5-keV  $E2$  transition from the  $12^+$  state to the  $10_2^+$  level, presumably the lower-spin member of the aligned band, has a strength of 9.7(26) W.u., while the competing 445.7-keV  $E2$  to the  $10_1^+$  state of the ground-state band is much weaker, at  $4.4(9) \times 10^{-2}$  W.u. The strength of the  $20^+ \rightarrow 18^+$ , 85.3-keV transition is close to one single-particle unit. The 111.5- and 85.3-keV  $\gamma$  rays at the point of the first and second alignments are essentially collective transitions, but modified by the change in wave function caused by the alignment gain.

Although various intrinsic states are predicted by the calculations in the same energy region, the structures observed do not have the associated rotational bands that would be expected if they were high- $K$  states. As indicated already, the current conclusion is that the observed  $20^+$ , 295-ns and  $12^+$ , 2-ns isomers in

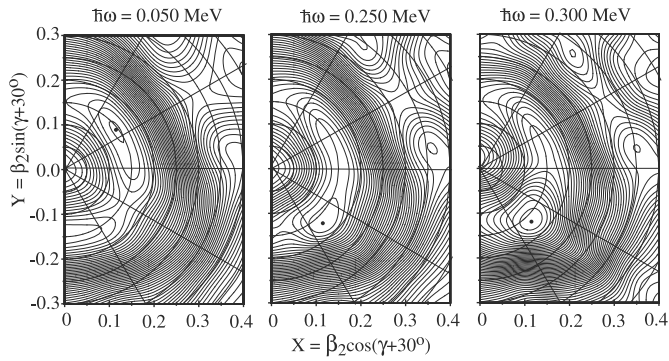


Fig. 4. Total Routhian surfaces for  $^{192}\text{Os}$  at the rotational frequencies indicated. The contour separation is 200 keV.

$^{192}\text{Os}$  are products of alignment gains within the set of  $i_{13/2}$  neutron orbitals at oblate deformation.

The dynamical effects and deformation changes supporting this conclusion are contained implicitly in the Total Routhian Surface (TRS) results given in Fig. 4, calculated using the approach detailed in Ref. [13]. The ground-state configuration is associated with a soft prolate deformation at low frequency (left panel) while the change towards oblate deformation (minimum at  $\gamma = -76^\circ$ ) is associated with about  $12\hbar$  of alignment from neutrons (middle panel). (See [13] for a similar prediction for the first neutron alignment in  $^{192}\text{Os}$  and  $^{190}\text{W}$ .) At higher frequencies, the deformation is similar but more localised (right-hand panel). However, from the wave functions, the total aligned angular momentum now has a component of about  $10\hbar$  from the protons, indicating that the second alignment is probably from the  $ab$  protons rather than the next pair of  $i_{13/2}$  neutrons ( $CD$ ).

This scenario of oblate deformation and consequent rotation alignment provides a consistent interpretation of the new results. However, it also opens up the question of the existence of competing high- $K$  multi-quasiparticle states such as a four-quasineutron  $20^+$  level from the  $11/2^+[615]$ ,  $13/2^+[606]$ ,  $7/2^- [503]$ ,  $9/2^- [505]$  prolate configuration predicted to lie at 4040 keV. To date, only the  $10^-$ , two-neutron (prolate) state has been identified, although in  $^{190}\text{Os}$ , a  $K^\pi = 7^-$  isomer from the  $\nu 3/2^- [512]$ ,  $11/2^+ [615]$  prolate Nilsson configuration has been assigned, in addition to its  $10^-$  isomer [30].

As pointed out in [21] in the context of possible  $35/2^-$  states in the Ir isotopes, the proximity of the neutron Fermi level to the  $11/2^+[615]$  and  $13/2^+[606]$  orbitals at prolate deformation means that configurations involving a pair of  $i_{13/2}$  neutrons coupled to  $J = 12^+$  should be favoured in energy. Fig. 5 presents the osmium level systematics obtained here from configuration-constrained potential-energy-surface calculations, related to those carried out for the iridium isotopes [21] (see Ref. [22] for similar calculations for  $^{188}\text{Os}$ ). Note that each level in this figure has been obtained from an independent minimisation with respect to the parameters describing the deformation. It can be seen from Fig. 5 that the  $12^+$  state is expected to fall almost linearly, to the extent that in  $^{194}\text{Os}$ , it would lie below any states to which it could reasonably decay. The related  $18^+$  state produced by coupling the  $3/2^- [512]$  and  $9/2^- [503]$  neutrons to the  $12^+$ ,  $i_{13/2}^2$  configuration is predicted to follow a parallel energy trajectory.

If these ( $12^+$  and  $18^+$ ) states indeed exist, they should be strongly populated since they would be nearly yrast. The calculations place the  $12^+$  state in  $^{192}\text{Os}$  just above the  $10^-$  intrinsic level, which would allow a (slow)  $M2$   $\gamma$ -ray decay to proceed. It is also above a predicted  $10^+$  state from the  $\pi 11/2^- [505]$ ,  $9/2^- [514]$  two-proton configuration that it could also decay to, al-

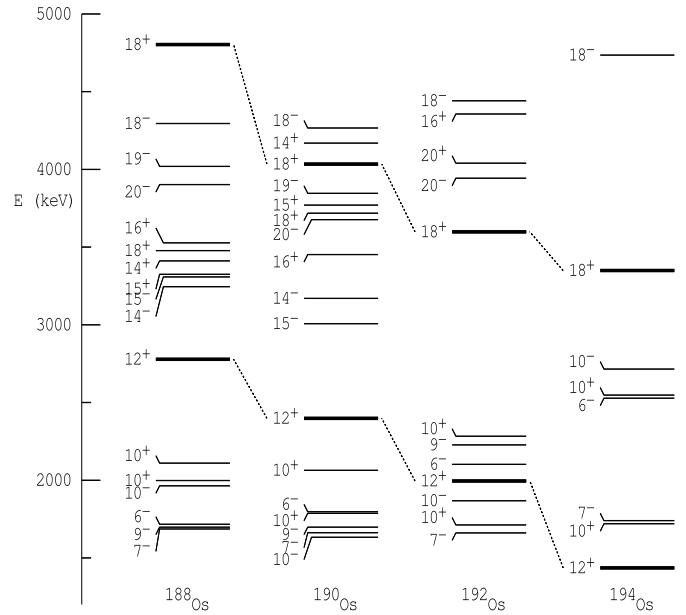


Fig. 5. Predicted multi-quasiparticle state energies calculated using configuration-constrained potential-energy-surfaces. Note that each level has been independently minimised.

beit via a slow  $E2$  transition, although this  $\pi^2$  state has not been observed in any of the isotopes under discussion. In  $^{194}\text{Os}$ , only  $\beta$ -decay is likely to be available. Note that the equilibrium deformations imply asymmetries close to  $30^\circ$  for states from both the  $10^+$  and  $12^+$  configurations. In fact, the calculated deformation parameters for the  $12^+$  states are very similar across this range of isotopes with  $\epsilon_2 = 0.15$ ,  $\epsilon_4 = -0.03$  and  $\gamma = 32^\circ$ . In contrast, the  $10^-$  two-neutron configuration has a  $\gamma$  value of  $20^\circ$  in  $^{188}\text{Os}$  and  $^{194}\text{Os}$ , but is predicted to be prolate ( $\gamma = 0^\circ$ ) in both  $^{190}\text{Os}$  and  $^{192}\text{Os}$ , consistent with the absence of signature splitting in the newly observed  $10^-$  band in  $^{192}\text{Os}$ .

Preliminary searches in the existing data for such decays have not been successful. Presumably, they would be evidenced by long-lived components in the population of excited states in the neighbours: in the case of  $^{192}\text{Os}$ , for example, our measurements would not be sensitive to a delayed single-step  $\gamma$ -ray decay to the  $10^-$  isomer, while  $\beta$ -decay would be to levels in  $^{192}\text{Ir}$ , as might be the case for the decay of the  $10^-$  isomer itself. The experimental issue is that such decays do not necessarily have a simple signature. For example, there is very little information on high-spin states in the daughter  $^{192}\text{Ir}$  and the most likely decay path would be to the 168-keV,  $11^-$  isomer which is essentially stable, with  $T_{1/2} = 241$  yr.

To summarise, new spectroscopic information for  $^{192}\text{Os}$  reveals states with properties that can be understood as the result of alignments within the high- $j$  neutron and proton orbitals at oblate deformation. Isomeric states occur, due largely to the low energies of connecting  $E2$  transitions. Such low energies arise because the combination of moderate oblate deformation and consequent proximity to very low- $\Omega$  orbitals, results in maximal alignment. An important experimental aspect has been the identification, using time correlations, of feeding through the high-spin states in  $^{192}\text{Os}$  that effectively bypasses the main low-spin yrast sequence and exposes the  $K^\pi = 10^-$  rotational band.

Configuration-constrained potential-energy-surface calculations also predict that other prolate and triaxial multi-quasiparticle structures should exist. Except for the  $10^-$  isomer, information on these remains very limited. The calculations suggest further,

that the favoured  $K = 12^+$  two-neutron configuration, which falls rapidly in energy with neutron number, will lead to low-lying intrinsic states, so low in  $^{194}\text{Os}$ , for example, as to be forced to  $\beta$ -decay. These and related states predicted in the iridium nuclei provide a challenge for future experimental studies, and for the understanding of configuration-dependent shapes and the competing dynamics in transitional nuclei.

### Acknowledgements

We are grateful to R.B. Turkentine for preparing the osmium targets. This work was supported by the Australian Research Council and the U.S. Department of Energy, Office of Nuclear Physics, under Contract No. DE-AC02-06CH11357 and Grant No. DE-FG02-94ER40848.

### References

- [1] C.Y. Wu, et al., Nucl. Phys. A 607 (1996) 178.
- [2] C.Y. Wu, D. Cline, Phys. Rev. 54 (1996) 2356.
- [3] D. Cline, Ann. Rev. Nucl. Part. Sci. 36 (1986) 683.
- [4] G. Thiamova, Eur. Phys. J. A 45 (2010) 81.
- [5] J.M. Allmond, R. Zaballa, A.M. Oros-Peusquens, W.D. Kulp, J.L. Wood, Phys. Rev. C 78 (2008) 014302.
- [6] C. Bihari, Y. Singh, M. Singh, A.K. Varshney, K.K. Gupta, D.K. Gupta, Phys. Scr. 78 (2008) 045201.
- [7] A.A. Raduta, P. Buganu, Phys. Rev. C 83 (2011) 034313.
- [8] P.D. Stevenson, M.P. Brine, Zs. Podolyak, P.H. Regan, P.M. Walker, J. Rikovska-Stone Phys. Rev. C 72 (2005) 047303.
- [9] P. Sarriguren, R. Rodriguez-Guzman, L.M. Robledo, Phys. Rev. C 77 (2008) 064322.
- [10] L.M. Robledo, R. Rodriguez-Guzman, P. Sarriguren, J. Phys. G 36 (2009) 115104.
- [11] R. Fossion, D. Bonatsos, G.A. Lalazissis, Phys. Rev. C 73 (2006) 044310.
- [12] K. Nomura, T. Otsuka, R. Rodriguez-Guzman, L.M. Robledo, P. Sarriguren, P.H. Regan, P.D. Stevenson, Zs. Podolyak, Phys. Rev. C 83 (2011) 054303.
- [13] P.M. Walker, F.R. Xu, Phys. Lett. B 635 (2006) 286.
- [14] G.D. Dracoulis, in: Proceedings of the Nobel Symposium on Physics with Radioactive Ion Beams, in: Phys. Scr. T, vol. 152, 2013, p. 014015.
- [15] P.M. Walker, G.D. Dracoulis, Nature 399 (1999) 35.
- [16] T. Kibédi, et al., Nucl. Instrum. Methods A 589 (2008) 202.
- [17] G.D. Dracoulis, et al., Phys. Rev. Lett. 97 (2006) 122501.
- [18] B. Singh, Nucl. Data Sheets 99 (2003) 275.
- [19] C.M. Baglin, Nucl. Data Sheets 113 (2012) 1871.
- [20] G.J. Lane, et al., Phys. Rev. C 82 (2010) 051304(R).
- [21] G.D. Dracoulis, et al., Phys. Lett. B 709 (59) (2012).
- [22] V. Modamio, et al., Phys. Rev. C 79 (2009) 024310.
- [23] S. Mohammadi, et al., Int. J. Mod. Phys. E 15 (2006) 1797.
- [24] C. Wheldon, J. Garces Narro, C.J. Pearson, P.H. Regan, Zs. Podolyak, D.D. Warner, P. Fallon, A.O. Macchiavelli, M. Cromaz, Phys. Rev. C 63 (2001) 011304.
- [25] P.H. Regan, et al., in: J. Jolie, A. Zilges, N. Warr, A. Blazhev (Eds.), Proc. 13th Intern. Symposium on Capture Gamma-Ray Spectroscopy and Related Topics, Cologne, Germany, 25–29 August 2008, in: AIP Conf. Proc., vol. 1090, 2009, p. 122.
- [26] N. Al-Dahan, et al., Phys. Rev. C 85 (2012) 034301.
- [27] Zs. Podolyak, et al., Phys. Rev. C 79 (2009) 031305.
- [28] J.J. Valiente-Dobon, et al., Phys. Rev. C 69 (2004) 024316.
- [29] R.V.F. Janssens, F.S. Stephens, Nucl. Phys. News 6 (1996) 9.
- [30] G.D. Dracoulis, et al., in press.
- [31] G.A. Jones, et al., Acta Phys. Pol., B 36 (2005) 1323.
- [32] D. Mehta, et al., Z. Phys. A 339 (1991) 317.
- [33] R. Bengtsson, S. Frauendorf, F.-R. May, At. Data Nucl. Data Tables 35 (1986) 15.
- [34] A.I. Levon, Yu.V. Nosenko, V.A. Onischuk, A.A. Schevchuk, A.E. Stuchbery, Nucl. Phys. A 764 (2006) 24.
- [35] G.D. Dracoulis, et al., in: Proceedings of the Rutherford Centennial Conference on Nuclear Physics, 8–12 August 2011, in: J. Phys. Conf. Ser., vol. 381, 2012, p. 012060.